



# Enhanced mesophilic anaerobic digestion of waste sludge with the iron nanoparticles addition and kinetic analysis

Yanru Zhang<sup>a,b</sup>, Zhaohui Yang<sup>a,b,\*</sup>, Rui Xu<sup>a,b</sup>, Yiping Xiang<sup>a,b</sup>, Meiyong Jia<sup>a,b</sup>, Jiahui Hu<sup>a,b</sup>, Yue Zheng<sup>c</sup>, WeiPing Xiong<sup>a,b</sup>, Jiao Cao<sup>a,b</sup>

<sup>a</sup> College of Environmental Science and Engineering, Hunan University, Changsha 410082, China

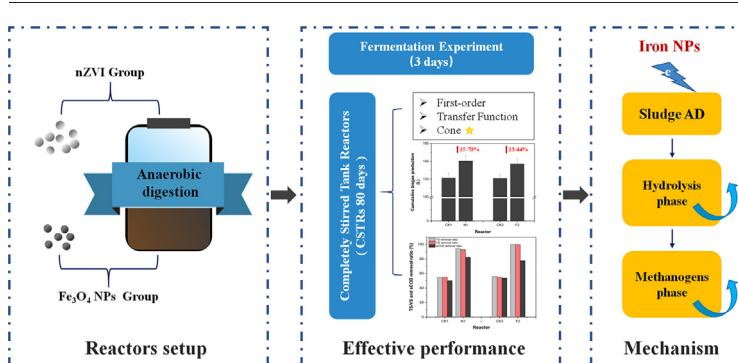
<sup>b</sup> Key Laboratory of Environmental Biology and Pollution Control (Hunan University), Ministry of Education, Changsha 410082, China

<sup>c</sup> CAS Key Laboratory of Urban Pollutant Conversion, Institute of Urban Environment, Chinese Academy of Sciences, Xiamen, 361021, China

## HIGHLIGHTS

- Addition of nZVI and Fe<sub>3</sub>O<sub>4</sub> NPs upgraded the sludge biogas production.
- The optimum dosage for biogas generation was 0.5 g L<sup>-1</sup> of nZVI and 1 g L<sup>-1</sup> of Fe<sub>3</sub>O<sub>4</sub> NPs.
- nZVI and Fe<sub>3</sub>O<sub>4</sub> NPs improved the sCOD and VS removal efficiencies.
- nZVI and Fe<sub>3</sub>O<sub>4</sub> NPs promoted the hydrolysis-acidification process of the sludge.
- Cone model best fitted the biogas results in AD with iron nanoparticles addition.

## GRAPHICAL ABSTRACT



## ARTICLE INFO

### Article history:

Received 23 March 2019

Received in revised form 14 May 2019

Accepted 14 May 2019

Available online 19 May 2019

Editor: Kevin V Thomas

### Keywords:

Anaerobic digestion

Mesophilic

Kinetic model

Nano zero-valent iron

Fe<sub>3</sub>O<sub>4</sub> nanoparticles

## ABSTRACT

As the functional material, iron nanoparticles effectively promote anaerobic digestion (AD) process, including the hydrolysis-acidification process and the biogas production. In this study, nano zero-valent iron (nZVI) and Fe<sub>3</sub>O<sub>4</sub> nanoparticles (Fe<sub>3</sub>O<sub>4</sub> NPs) were added to AD reactors respectively. The AD process was evaluated by the reactors performances, including pH, biogas yields and compositions, as well as the removal ratio of total solids (TS), volatile solids (VS) and soluble chemical oxygen demand (sCOD). Three models (first-order kinetic model, transfer function model and Cone model) were used to explore the kinetics of AD biogas production. The results showed that adding appropriate dose of nZVI or Fe<sub>3</sub>O<sub>4</sub> NPs enhanced anaerobic digestibility of sludge. The highest cumulative biogas yield of 140.34 L with 0.5 g L<sup>-1</sup> nZVI and 137.13 L with 1 g L<sup>-1</sup> Fe<sub>3</sub>O<sub>4</sub> NPs were obtained by the 80 days of mesophilic operation, respectively. Cumulative biogas productions of these two reactors were significantly enhanced up to 15.70% and 13.44%. TS removal rates reached >70% in all AD reactors with iron nanoparticles, and the highest sCOD removal rates of nZVI and Fe<sub>3</sub>O<sub>4</sub> NPs digesters on the 80th day were 88.22% and 77.63%, respectively. The results of the three-day fermentation experiment and the kinetic parameters showed that the nZVI or Fe<sub>3</sub>O<sub>4</sub> NPs enhanced the hydrolysis-acidification process of the AD, which eventually promoted biogas production. The Cone model was satisfied with the experimental results, which could be used to evaluate the kinetics of AD with iron nanoparticles more reasonably.

© 2019 Elsevier B.V. All rights reserved.

\* Corresponding author at: College of Environmental Science and Engineering, Hunan University, Changsha 410082, China.  
E-mail address: [yzh@hnu.edu.cn](mailto:yzh@hnu.edu.cn) (Z. Yang).

## 1. Introduction

Due to the overuse and exhaustion of fossil fuels, the world, especially China, is confronted with the grave energy shortage crisis. Developing new resources and making full use of sustainable energy have become imminent. Sewage sludge is not only a common municipal waste but also a neglected resource. In China, the annual production of dried sludge is >11.2 million tons, while the innocuous disposal rate of sludge is only 25.1%, and >80% of sludge is dumped without necessary stable treatment (Yang et al., 2015). The management methods of sludge reutilization, harmlessness and reduction have attracted the particular attention of governments and scholars to the entire world.

Anaerobic digestion (AD) is a technology for degrading the matrix organic matter by various species of microorganisms under anoxic conditions (Xu et al., 2018a; Xu et al., 2017; Zhen et al., 2016). AD is extensively used to reduce the organism and the pathogenic from waste activated sludge (WAS), especially in large wastewater treatment plants (WWTPs). The clean energy produced by AD is an available and cost-effective alternative to fossil fuels. Furthermore, renewable energy is recovered in the form of biogas (mainly composed of CO<sub>2</sub> and CH<sub>4</sub>) (Gang et al., 2013). However, the restrictive steps of hydrolysis and the high inhibition of ammonium reduce the hydrolysis rate and methane production, which limit the economic viability of AD (Ferreira et al., 2014). To improve the economics of biogas production, scholars have studied different ways to increase biogas yield. Pretreatment, co-digestion, electrochemical binding, and using additives are all interesting techniques for stimulating the growth of methanogens and reducing the inhibition of ammonia concentration (Ahmadi-Pirlou et al., 2017). Notably, adding iron nanoparticles to AD can accelerate the hydrolysis-acidification process, increase methane production and stabilize the sludge (Feng et al., 2014; Li et al., 2014).

Because many bacteria have developed pathways to obtain iron in the form of nutrients or electronic acceptor/donor, the iron is vital to the living organisms (Melton et al., 2014). As a non-toxic, abundant and inexpensive iron nanoparticle, nano zero-valent iron (nZVI) has created an enhanced anaerobic environment with low H<sub>2</sub> content (or partial pressure) as well as low oxidation-reduction potential after being added to the anaerobic digestive system (Hu et al., 2015). As the electron donors for AD system, nZVI can not only accelerate sludge hydrolysis-acidogenesis but also change the fermentation type to increase the acetic acid concentration and ultimately promote methane yield (Pan et al., 2019). By directly or indirectly donating electron (H<sub>2</sub>/[H]), nZVI can advance the metabolism and growth of critical microorganisms (such as methanogens) in the anaerobic process. Meanwhile, iron is provided as a trace element to enhance the activity and abundance of hydrogen-consuming microbes (Wei et al., 2018; Yaobin et al., 2011).

Fe<sub>3</sub>O<sub>4</sub> nanoparticles (Fe<sub>3</sub>O<sub>4</sub> NPs) is a mixed valence magnetic mineral containing both Fe<sup>2+</sup> and Fe<sup>3+</sup> in a proportion of 1:2 (Byrne et al., 2015). The positive effect of Fe<sup>2+</sup> on methanogenesis is recognized since Fe<sub>3</sub>O<sub>4</sub> NPs increased methanogenic activity associated with accelerated organic degradation. Fe<sub>3</sub>O<sub>4</sub> NPs has also been proved to advance methane production by promoting direct interspecies electron transfer (DIET) in syntrophic methanogenesis (Li et al., 2014). DIET is a relatively novel electron delivery route discovered in recent decades and has been widely proved in anaerobic systems, such as paddy soils, bio-electrochemical anaerobiosis and anaerobic digestion reactors (McGlynn et al., 2015). Microbial nanowires directly transfer electrons generated by intermediates from syntrophic bacteria to methanogenic archaea. Archaea used the electrons obtained to reduce carbon dioxide (CO<sub>2</sub>) and ultimately produces methane (Rotaru et al., 2013). DIET occurred in the presence of Fe<sub>3</sub>O<sub>4</sub> NPs can be used as an alternative to microbial nanowires for enhancing methane production remarkably by effectively transferring electrons (Li et al., 2014) and accelerating methane synthesis of from butyrate (Barua and Dhar, 2017). Fe<sub>3</sub>O<sub>4</sub> NPs are abundant in quantity and have good conductive properties, but few studies have been done on the ability to DIET in the complex anaerobic digestive sewage sludge.

Kinetic modeling is of great significance for exploring the stability of AD process performance, understanding the rising curve of biogas production, predicting and optimizing the process of AD system (Mao et al., 2017). Moreover, different modeling parameters provide a good understanding to the biological reaction mechanism of AD, reduce the time of laborious experiments required and help researchers to obtain desired simulated results (Xie et al., 2016). We can explore the influence of the addition of iron nanoparticles on the key parameters of the anaerobic digestion reactors combined with the biogas generation kinetics, including the ultimate maximum biogas yield, hydrolysis rate, maximum biogas production rate and lag phase. Some studies have reported the methane produce kinetics from the anaerobic co-digestion of different agricultural waste (Hassan et al., 2017; Li et al., 2015). However, most of the studies simulate the discontinuous anaerobic digestion process basing on the first-order model or the modified Gompertz model. Very few papers used other models such as the transfer function model and the Cone model. The reliability of the above models is difficult to control because of changing kinetic parameters, which affected by operational conditions and experimental environment. To the best of our knowledge, nZVI and Fe<sub>3</sub>O<sub>4</sub> NPs have the potential to enhance biogas yield, but there are still knowledge vacancies in the kinetic information for AD with nZVI or Fe<sub>3</sub>O<sub>4</sub> NPs. The kinetics of biogas production from the different dose of nZVI or Fe<sub>3</sub>O<sub>4</sub> NPs which use three kinetic models including first-order kinetic model, transfer function model and cone model under the completely stirred tank reactors (CSTRs) has not been reported. It is also necessary to carefully compare different kinetic models of AD with iron nanoparticles addition.

A certain amount of iron nanoparticles can increase the biogas yield of the sludge AD system. However, the methanogenic effect of the system will decrease when the iron nanoparticles dosage exceeds the tolerance range of the methanogen (Yang et al., 2013). Until now, the role of iron nanoparticles in AD systems is still uncertain, sometimes even contrary. The questions still exist regarding how iron nanoparticles will affect anaerobic processes such as hydrolysis, acidogenesis and methanogenesis. Based on the above considerations, four different dosages of nZVI or Fe<sub>3</sub>O<sub>4</sub> NPs were thus performed herein in a series of CSTR experimentations, and three classic kinetic models (first-order kinetic, transfer function and Cone models) were selected to fit the biogas yield data of the AD reactors in our study. The purpose of this research is to i) evaluate the biogas yield and feasibility of mesophilic CSTRs with nZVI or Fe<sub>3</sub>O<sub>4</sub> NPs addition, ii) explore the exact roles of nZVI or Fe<sub>3</sub>O<sub>4</sub> NPs in AD process and iii) estimate the three kinetic models for biogas prediction and to calculate the kinetic parameters using the measured biogas data in practical experiments. The purpose of this study is to develop a sustainable sludge stabilization strategy and achieve bio-energy recovery.

## 2. Materials and methods

### 2.1. Sludge and iron nanoparticles

AD reactors were inoculated with 2 L inoculum and 1 L substrate. The inoculum was collected from a mature mesophilic anaerobic digester. The substrate, a mixture of dewatered sludge and secondary sludge, was collected from the Second Wastewater Treatment Plant, Changsha, China. Table 1 showed the analysis results of substrates and inoculums physico-chemical properties in triplicates. The iron nanoparticles employed were nZVI (diameter of 50 nm, purity 99.9%) and Fe<sub>3</sub>O<sub>4</sub> NPs, (diameter of 20 nm, purity >99.5%), respectively, which were both purchased from Macklin biochemical technology co. LTD, Shanghai, China.

### 2.2. Experimental equipment and operation of semi-continuous anaerobic digestion

The batch experiment and the long-term semi-continuous experiment were carried out to explore the influence of nZVI and Fe<sub>3</sub>O<sub>4</sub> NPs

**Table 1**  
Characteristics of substrate and inoculum sludge used in the experiment\*.

Parameter	Substrate	Inoculum
Volume (mL d <sup>-1</sup> )	150.00	/
pH	7.17 ± 0.005	6.79 ± 0.015
Moisture (%)	91.84 ± 0.089	98.45 ± 0.056
TS (%)	8.16 ± 0.089	1.54 ± 0.056
VS (%)	4.77 ± 0.059	0.79 ± 0.00
sCOD (g L <sup>-1</sup> )	9.47 ± 0.033	0.44 ± 0.042
NH <sub>4</sub> <sup>+</sup> -N (mg L <sup>-1</sup> )	65,804.93 ± 4341.98	29,101.08 ± 792.98

\* The data reported are the averages and their standard deviations in triplicate tests.

on hydrolysis-acidification process and methanogenesis process respectively. The experiment was set as the nZVI group and the Fe<sub>3</sub>O<sub>4</sub> NPs group. Five reactors of nZVI group were set up: [Blank (CK1), with nZVI [N1 (0.5 g L<sup>-1</sup>), N2 (1 g L<sup>-1</sup>), N3 (2 g L<sup>-1</sup>), N4 (4 g L<sup>-1</sup>)] and five reactors for Fe<sub>3</sub>O<sub>4</sub> NPs group: Blank (CK2), with Fe<sub>3</sub>O<sub>4</sub> NPs [F1 (0.5 g L<sup>-1</sup>), F2 (1 g L<sup>-1</sup>), F3 (2 g L<sup>-1</sup>), F4 (4 g L<sup>-1</sup>)]. Three parallel samples were set for each reactor.

The long-term semi-continuous experiment was carried out in CSTRs to study the effect of nZVI or Fe<sub>3</sub>O<sub>4</sub> NPs on the whole anaerobic process including hydrolysis-acidification and methanogenesis. The experimental reactor consisted of an organic glass reactor with a working volume of 3 L and two gas collection bottles with 5 L total volume. The top of the plexiglass reaction bottle was set up with a rubber plug, which fitted with the feed/discharge port and the gas outlet. CSTRs were operated at a constant feed rate of 150 mL day<sup>-1</sup> for 80 days with a hydraulic retention time (HRT) of 20 days. CSTRs system temperature was controlled under mesophilic conditions (35.0 ± 2 °C) by a water bath.

The batch experiment lasted only for three days to investigate the influence of nZVI and Fe<sub>3</sub>O<sub>4</sub> NPs on hydrolysis-acidification. In the serum bottles with 300 mL working volume, the mixture sludge including 200 mL inoculum and 100 mL substrate was heat-treated. Adding 2-bromoethane sulfonic acid (BESA) to the mixture sludge can efficiently get rid of methanogens from anaerobic fermentation system. The operation method of this experiment is reported in the literature (Feng et al., 2014). After the pretreatment of mixture sludge, the batch experiment was operated under the same conditions as the long-term semi-continuous experiment. All the experiments were conducted in triplicate.

### 2.3. Sample collection and analytic methods

The daily biogases produced by the CSTRs were determined by saturated salt water-replace method, and the same volumes of saturated salt water were pressed into the collector. The produced biogases on the 80th day were collected with the gas collecting bag. Gas-tight syringe (1 mL injection volume) and Shimadzu Gas Chromatograph (GC 2010, Japan) equipped with a thermal conductivity detector were used to determine the biogas components (mainly methane and carbon dioxide).

Measurements of pH, moisture, total solids (TS), volatile solids (VS), soluble chemical oxygen demand (sCOD), total polysaccharide and NH<sub>4</sub><sup>+</sup>-N were performed according to the Standard Methods (Eaton, 2005). These analytics methods have been introduced in our previous researches (Xu et al., 2018b; Yang et al., 2016).

### 2.4. Kinetic models

Three different kinetic models, i.e., the first-order kinetic, transfer function, and Cone model, were shown in Table 2. These models described the kinetic parameters of biogas yield. The first-order kinetic model (Eq. (1)) takes the substrate utilization as the limiting factor and presumes that hydrolysis manages the overall process. This model, however, can neither calculate the biogas yield rate nor evaluate the lag phase (Li et al., 2015). Transfer function model (Eq. (2)) analyzes the anaerobic digestion process as a system for receiving inputs and

generating outputs. This model predicts the maximum biogas yield according to cumulative biogas production with time-variation (Li et al., 2012). The formula of the transfer function model could be used to calculate biogas production potential, as well as provide maximum biogas production rate and duration of lag phase. Cone model (Eq. (3)) as an empiric model that can identify the biogas yield rate and maximum cumulative biogas yield. Moreover, the Cone model can also estimate the biogas production behavior by the shape constant, which reveals whether there is a lag phase in the reactors.

### 2.5. Models evaluation and validation

This study calculated the correlation coefficients (R<sup>2</sup>), Root Mean Square Prediction Error (rMSPE) (Eq. (4)) and Akaike's Information Criterion (AIC) (Eq. (5)), which were used to compare the three models.

(1) R<sup>2</sup>, also called the fitness index, was decided by the Origin 2015 software.

(2) The rMSPE value indicates the standard deviation between predicted and measured values. The lower rMSPE value demonstrates the better model fitting. The calculation of rMSPE was described as below (Wang et al., 2011):

$$rMSPE = \sqrt{\frac{\sum_{i=1}^n (P_{vi} - M_{vi})^2}{n}} \quad (4)$$

Where  $P_{vi}$  is the predicted value of biogas yield,  $M_{vi}$  is the measured value of biogas yield, while  $n$  is the number of measurements.

(3) AIC is an alternative method based on information technology development to compare nested and non-nested models. It is used to compare models and determine which model is more suitable for practical experiments. The model with lower AIC value is more likely to be suitable than the model with higher AIC value (Christopoulos, 2006). The formula for calculating AIC was as below:

$$AIC = n \ln \left( \frac{RSS}{n} \right) + 2(N + 1) + \frac{2(N + 1)(N + 2)}{(n - N - 2)} \quad (5)$$

Where  $RSS$  is the residual sum of squares,  $n$  is the number of measurements, and  $N$  is the number of model parameters.

### 2.6. Statistical analysis

SPSS statistics 19.0 software was used to analyze variance (ANOVA) for the results obtained during different conditions and the results were expressed as mean ± standard deviation. All assays were carried out in triplicate. The parameters such as cumulative biogas production ( $B_0$ ), hydrolysis rate ( $k$ ), maximum biogas production rate ( $R_m$ ), lag phase ( $\lambda$ ), and shape factor ( $n$ ) were calculated by fitting the measured biogas data into the kinetic models through the software Origin 2015. The software Origin 2015 was also used to produce graphs.

## 3. Results and discussion

### 3.1. Physicochemical properties of substrates and inoculums

The pH values of substrate and inoculum were 7.17 and 6.79 respectively, which were beneficial to maintain the stability of the AD system. The substrate sludge based on a percentage of the "safe" TS at 8.16% and had VS content of 4.77%. The relatively low organic content is the largest characteristic of Chinese sludge. The substrate sludge TS content in this experiment was similar to that reported by (Budiyo, 2010), which is, the digestibility of cattle manure displays the best performance when the TS content is 7.4% to 9.2%. The sCOD content of substrate sludge was relatively high, about 9.47 g L<sup>-1</sup>. As for the inoculum sludge, it presented typical values of anaerobic sludge from municipal WWTP since

**Table 2**  
Models used to describe the kinetics of biogas production.

Model	Equation	Parameters	N
First-order kinetic model	$B_{(t)} = B_0[1 - \exp(-kt)]$ (1)	$B_0, k$	2
Transfer function model	$B_{(t)} = B_0 \{1 - \exp[-\frac{R_m(t-\lambda)}{B_0}]\}$ (2)	$B_0, R_m, \lambda$	3
Cone model	$B_{(t)} = \frac{B_0}{1 + (kt)^{-n}}$ (3)	$B_0, k, n$	3

Where  $B_{(t)}$  is the cumulative biogas yield at digestion time  $t$  (L);  $B_0$  represents the ultimate maximum biogas yield (L) of substrate;  $k$  stands for hydrolysis rate ( $d^{-1}$ ) and  $t$  is the digestion time (d);  $R_m$  is the maximum biogas production rate (L day $^{-1}$ );  $\lambda$  is the lag phase (d);  $n$  is the shape factor;  $e$  is  $\exp(1) = 2.7183$ , and  $N$  is the number of model parameters.

pH, TS (%), and VS (%) are indicative of good buffer capacity which favors anaerobic digestion (Patricia et al., 2009).

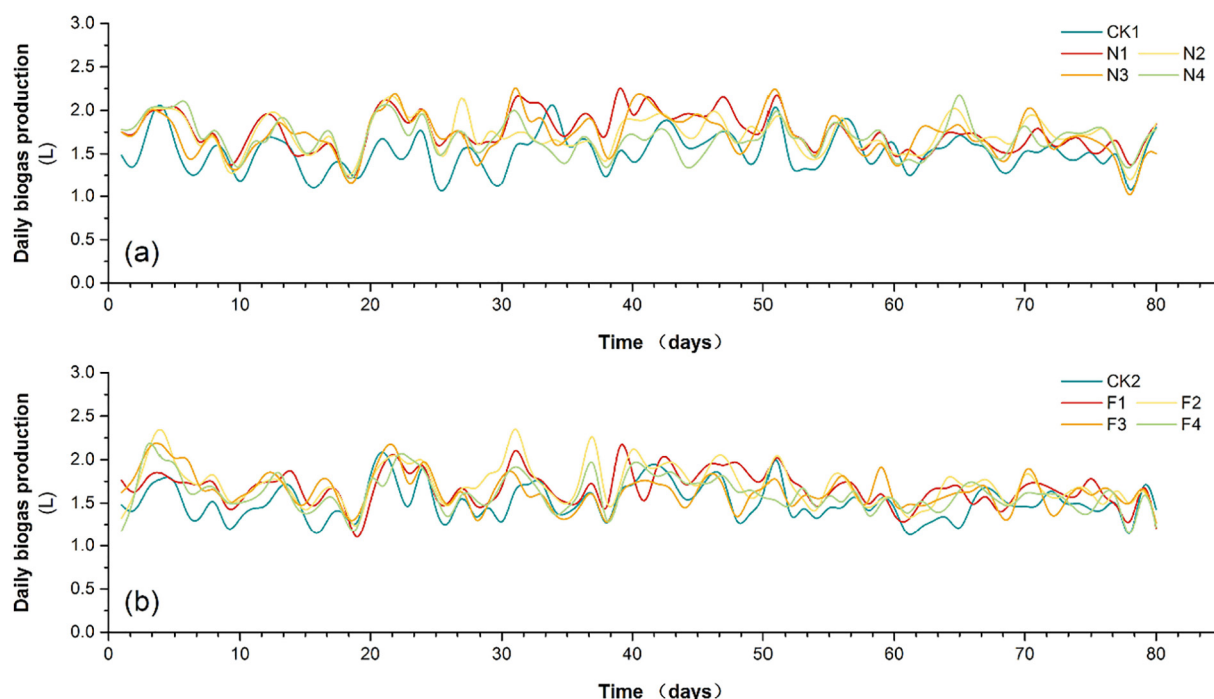
### 3.2. Changes in the biogas yield

Fig. 1 detailed the shifts in the daily biogas yield with distinct treatments during the 80-day CSTRs. In general, the range of daily biogas production fluctuated in 1–2.6 L. As shown in Fig. 2 (a), after digestion for 80 days, the amount of cumulative biogas generated varies because of different nZVI dosages, in the following order (from high to low): 0.5 g L $^{-1}$  (N1), 1 g L $^{-1}$  (N2), 2 g L $^{-1}$  (N3), 4 g L $^{-1}$  (N4), 0 g L $^{-1}$  (CK1). The range of cumulative biogas yields varied from 121.30 to 140.34 L. Adding 0.5 g L $^{-1}$  of nZVI (N1) could maximize the cumulative biogas yield of AD in this study. Compared to the CK1, the cumulative biogas yield was increased by 15.70% with N1. However, with the dosage of nZVI increased to 4 g L $^{-1}$  (N4), the cumulative biogas yield only accelerated 10.74% higher than that of the CK1. For the group with Fe $_3$ O $_4$  NPs in Fig. 2 (b), the cumulative biogas production in anaerobic fermentation showed a trend of increasing and followed by decreasing with the increase in Fe $_3$ O $_4$  NPs dosage. Under different Fe $_3$ O $_4$  NPs dosages, the order of cumulative biogas productions was roughly as follows: 1 g L $^{-1}$  (F2) > 0.5 g L $^{-1}$  (F1) > 2 g L $^{-1}$  (F3) > 4 g L $^{-1}$  (F4) > 0 g L $^{-1}$  (CK2) g L $^{-1}$ . The cumulative biogas yields ranged from 120.88 to 137.13 L in the Fe $_3$ O $_4$  NPs group, and 1 g L $^{-1}$  (F2) was the optimum dosage in this experiment, the relative cumulative biogas production rate accelerated by 13.44%.

In the data of cumulative biogas generation, there was a statistical difference between the reactor with iron nanoparticles and the reactor without iron nanoparticles ( $P < 0.05$ ). This result was consistent with earlier studies which suggested that adding nZVI or Fe $_3$ O $_4$  NPs could enhance methane production. However excessive nZVI addition can damage the integrity of cells and inhibit methane production. For example, Wu et al. (Wu et al., 2015) reported that the methane production was positively correlated with ZVI addition, while a high dosage of ZVI (>50 g L $^{-1}$ ) weakened the promotion of ZVI on the AD of swine wastewater. Some scholars also observed that methane yield rate increased by 44% as a result of the DIET promotions by Fe $_3$ O $_4$  NPs addition (Jing et al., 2017).

Notably, the biogas composition analysis (Fig. 3) showed that the addition of iron nanoparticles not only increased biogas production but also enhanced methane content. Concretely the CH $_4$  percentage in the biogas ranged from 62.41% to 64.97% in the case of nZVI group and the value ranged from 64.1% to 69.44% in the case of Fe $_3$ O $_4$  NPs group. The remaining biogas was mainly CO $_2$  while H $_2$  content was <1%. It is worth noting that CH $_4$  content also increased with the increase of Fe $_3$ O $_4$  NPs dosage. In the reactor with the Fe $_3$ O $_4$  NPs dosage of 4 g L $^{-1}$  (F4), the CH $_4$  content increased by 17.22%.

The methanogenesis process was carried out by the methanogenic archaea (Karve, 2003), which has the vital function on carbon cycling. The homeostasis of iron is essential for all life forms especially the archaea microorganisms. Iron ions (including Fe $^{2+}$  and Fe $^{3+}$ ) are fundamental in vital functions such as power generation and DNA replication. Iron ions released by iron nanoparticles can infiltrate into



**Fig. 1.** Daily biogas production from CSTRs of nZVI group (a) and Fe $_3$ O $_4$  NPs group (b) with different dose.



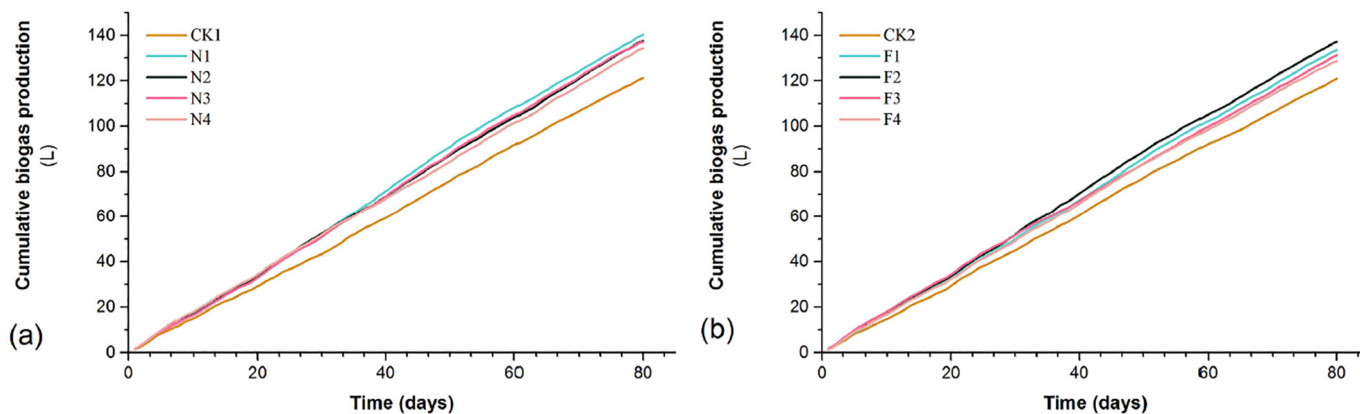


Fig. 2. Cumulative biogas production from CSTRs of nZVI group (a) and  $\text{Fe}_3\text{O}_4$  NPs group (b) with different dose.

the interior of cells and promote the synthesis of key enzymes and the growth of microorganism, especially methanogens (Zhen et al., 2015a). Due to the easiness to obtain or lose electrons, iron nanoparticles can be used as cytochrome and ferredoxin to participate in the energy metabolism of methyl-trophic methanogens and reduce  $\text{CO}_2$  to  $\text{CH}_4$  by autotrophic methanogenesis (Shen et al., 1993). Moreover, present study suggested that ZVI can directly enhance all steps involved in AD process (Xiao et al., 2013), i.e., hydrolysis, acidification and methanogenesis by stimulating the enzyme secretion and the microbial growth rate of hydrogen-consuming (Capson-Tojo et al., 2018). However, excessive ions can easily produce highly reactive and toxic free radicals that are harmful to different molecules (e.g., nucleic acids and lipids,) (Banfield and Zhang, 2001). Although iron is essential, it is toxic at higher concentrations, adding appropriate concentration of ions in the anaerobic reactor can increase biogas production. However, at a higher dosage, nZVI or  $\text{Fe}_3\text{O}_4$  NPs have a depressant effect on the AD process.

### 3.3. Biodegradability and stability performance of CSTRs

Except for biogas production behavior, the removal ratio of VS and sCOD as two important parameters were used to determine the anaerobic digestion efficiency (Zhen et al., 2016).

In general, the VS content in different treatment reactors showed a downward trend during the entire AD process. As shown in Fig. 4 (a) and (b), the VS concentrations of the CK1, N1, N2, N3, N4, CK2, F1,

F2, F3, and F4 digesters were 3.75%, 3.21%, 3.21%, 3.18%, 3.14%, 3.75%, 3.21%, 3.08%, 3.34%, and 3.34%, respectively. From Fig. 4 (c) and (d), the highest VS removal for N1 and F2 were observed (92.76% and 100% respectively). The TS/VS removal efficiencies decreased with the increase of nZVI dose.

Fig. 5 depicted the effects of nZVI and  $\text{Fe}_3\text{O}_4$  NPs on sCOD concentrations change in the 80-day experimentation. sCOD concentrations in the nZVI group (Fig. 5 (a)) were 82.22%, 78.29%, 67.25%, and 60.07%, while in the  $\text{Fe}_3\text{O}_4$  NPs group were 68.89%, 77.63%, 63.53%, and 62.75% (Fig. 5 (b)). The variation trend of sCOD concentration was similar to the trend of VS content. Compared with the control reactor (CK1 and CK2, respectively),  $0.5 \text{ g L}^{-1}$  nZVI (N1) and  $1 \text{ g L}^{-1}$   $\text{Fe}_3\text{O}_4$  NPs (F2) did cause positive influence on sCOD removal ratio with the sCOD removal ratio were 82.22% (N1) and 77.63% (F2) respectively.

The high removal rate of VS, TS and sCOD in added nZVI reactors indicated that nZVI could promote AD process and anaerobic microbial activity. A similar conclusion has been summarized in  $\text{Fe}_3\text{O}_4$  NPs added systems. Study shown that COD conversion rate is limited when the iron content is insufficient (Oleszkiewicz and Sharma, 1990). It may be based on the fact that nZVI and  $\text{Fe}_3\text{O}_4$  NPs can be used as electron donor and release  $\text{Fe}^{2+}$  into the anaerobic system, thereby accelerating the hydrolysis and fermentation process. Internal production including monomers, polypeptides, long and short chain fatty acids, alcohols and amino acids were generated in the hydrolysis and acidification steps of AD (Hassan et al., 2016). sCOD was the product of the hydrolysis and fermentation stages during the AD process, including soluble proteins,

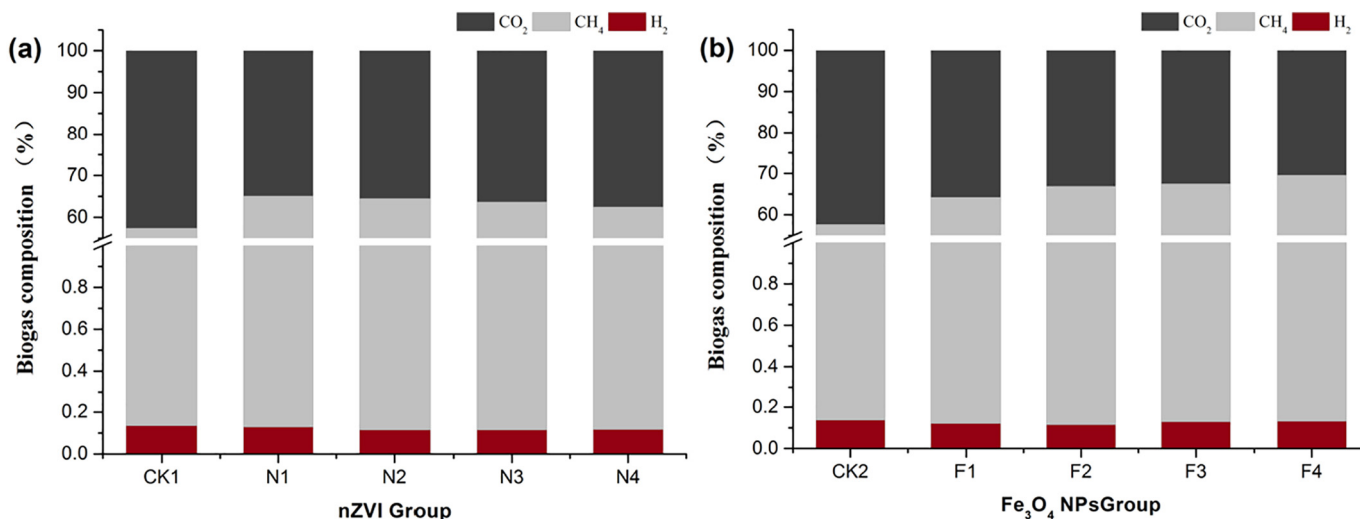


Fig. 3. Composition of biogas production in nZVI group (a) and  $\text{Fe}_3\text{O}_4$  NPs group (b) on day 80.

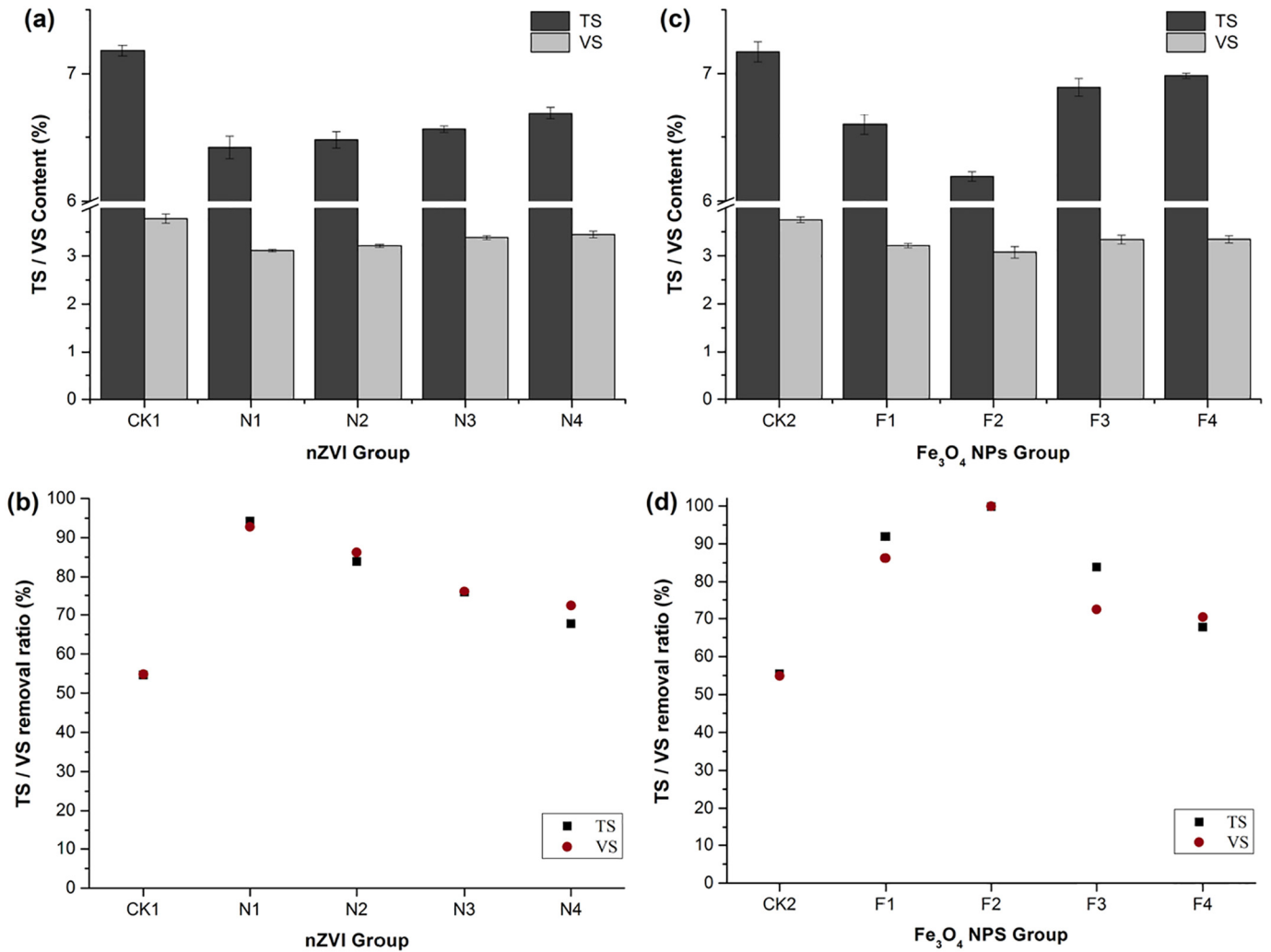


Fig. 4. TS/VS content and removal rate after CSTRs for 80 days under the nZVI group (a) and (c); the Fe<sub>3</sub>O<sub>4</sub> NPs group (b) and (d).

soluble polysaccharide and volatile fatty acids (VFAs). The reduction of organic components in sludge leads to methane production at the methanogenic stage. And the methane production is proportional to the consumption of these internal products such as methane-producing species which is also the significant indicator to measure the AD

performance. In general, the methane production was well-connected with the decrease of VS and sCOD within the digestate.

The operating state of AD could be reflected via the variations of pH value of digesters to some extent. From Fig. S1, the pH value of all reactors showed an overall upward trend, and finally stabilized around 7.75

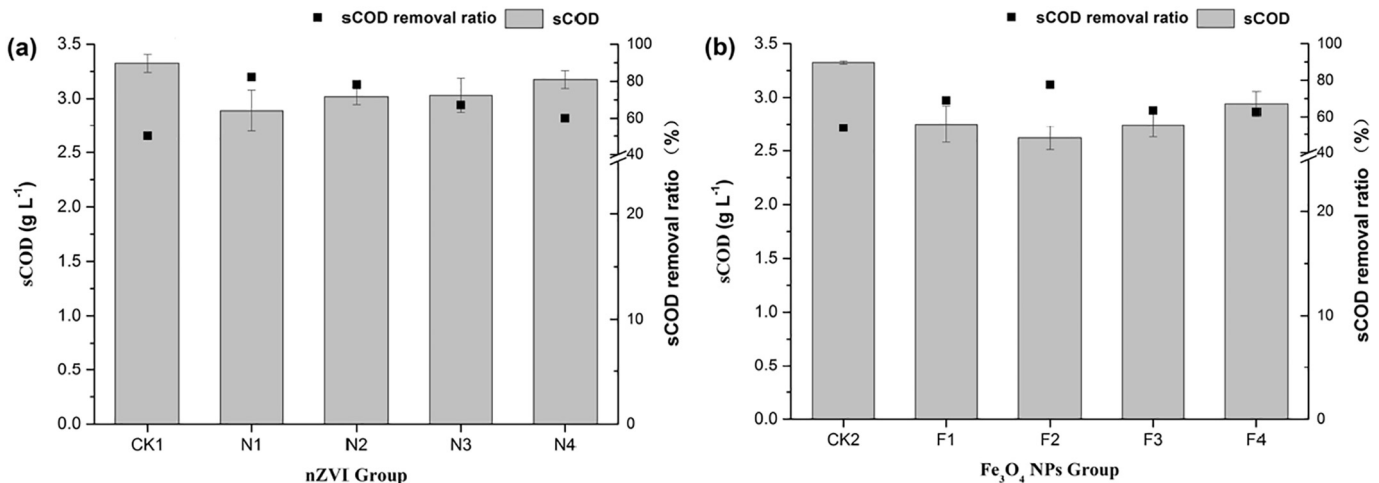


Fig. 5. sCOD content and removal rate after CSTRs for 80 days under the nZVI group (a) and the Fe<sub>3</sub>O<sub>4</sub> NPs group (b).

during the 80-day CSTRs. There was no significant difference ( $P > 0.05$ ) in pH between the reactors with iron nanoparticles added and the reactors without iron nanoparticles added, which indicated that the addition of iron nanoparticles would not significantly change the pH value of the reactor and the AD reactor could still maintain a relatively stable operating state.

Overall, the decrease of TS, VS and sCOD accumulation verified the improvement of the degradation ability in AD process with the addition of nZVI or  $\text{Fe}_3\text{O}_4$  NPs. The mechanism of nZVI and  $\text{Fe}_3\text{O}_4$  NPs promoting anaerobic fermentation of sludge will be discussed below.

### 3.4. Effect of nZVI and $\text{Fe}_3\text{O}_4$ NPs on the hydrolysis-acidification

The dosages of nZVI or  $\text{Fe}_3\text{O}_4$  NPs with 0, 0.5, 1, 2 and 4 g  $\text{L}^{-1}$  were added to five sludge digestion reactors pre-removed methanogens to reveal the influence of iron nanoparticles on the hydrolysis-acidification process. After three days of fermentation, the sCOD and total polysaccharide in the samples were measured. Fig. 6 showed the results. After the fermentation with nZVI or  $\text{Fe}_3\text{O}_4$  NPs for three days, the sCOD concentration of N2 in the nZVI group was the highest, and that of F2 in the  $\text{Fe}_3\text{O}_4$  NPs group was the highest. The sCOD concentration with no nZVI or  $\text{Fe}_3\text{O}_4$  NPs was the lowest, only 7.799 g  $\text{L}^{-1}$  for CK1 and 7.802 g  $\text{L}^{-1}$  for CK2. At reactors with iron nanoparticles added, the total polysaccharide reduced to 0.320, 0.319, 0.364 and 0.371 g  $\text{L}^{-1}$  in nZVI group and the value reduced to 0.345, 0.333, 0.343 and 0.371 g  $\text{L}^{-1}$  in  $\text{Fe}_3\text{O}_4$  NPs group. This result indicated that the decomposition rate of total polysaccharide was the highest at the dose of 1 g  $\text{L}^{-1}$  of nZVI or  $\text{Fe}_3\text{O}_4$  NPs, which is 21.75% and 15.82% higher than the control reactor, respectively. The decomposition of total polysaccharide at the N1 approached to that of N2.

The organics in sludge are mainly particulate matters before fermentation, which needs to convert into soluble compounds for utilization. After adding the nZVI to anaerobic fermentation digestors, the quantity of micro-electrolysis systems has been formed for disintegrating sludge matrix. More granular proteins and carbohydrates rapidly solubilized and hydrolyzed for later biological treatment. Micro-electrolysis is a valid method to improve the biodegradability of organic compounds in many studies. For example, Feng et al. (Feng et al., 2014) reported that nZVI available promoted the decomposition of two major sludge compositions, namely protein and total polysaccharide. The degradation of total polysaccharide increased by 29.6% with nZVI added in the hydrolysis-acidification experiment. Some reports also found that the fermenting bacteria, with responsibility for hydrolyzing sludge and producing VFAs in anaerobic fermentation digestors with nZVI, enriched to a high level. This phenomenon was consistent with the improvement of

sludge solubilization and hydrolysis as well as short-chain fatty acids (SCFAs) growth (Luo et al., 2014). It would be another reason for the growth in sCOD and the reduction in total polysaccharide on the hydrolysis-acidification process.

### 3.5. Kinetic study of biogas production

It is a necessary task to parameterize the model equations by fitting the measured experimental data. To calculate and compare the biogas yields during the AD process of nZVI and  $\text{Fe}_3\text{O}_4$  NPs, three mathematical models were used: the first-order model, transfer function model and Cone model. The calculated kinetic constants are exhibited in Table 3–5, respectively.

First of all, Table 3–5 showed that cumulative biogas yield was well fitted by all these three models, and the determination coefficient ( $R^2$ ) were all  $>0.999$ . The  $R^2$  values of the first-order kinetic (ranged from 0.9994 to 0.9999) and the transfer function (ranged from 0.9995 to 0.9999) models were lower than that of the Cone model (ranged from 0.9997 to 0.9999). On the other hand, as shown in Table 3–5, all the models have a difference of  $<1\%$ . The low calculated deviation (close to or  $<10\%$ ) between the predicted and measured values showed that the model used in this study could predict the reactors behavior reliably.

From the three models, it can be estimated that the  $B_0$  of the same reactor was almost similar. However, nZVI and  $\text{Fe}_3\text{O}_4$  NPs systems had different estimates of  $B_0$  under different dose. The predicted  $B_0$  obtained by the Cone model was closer to the measured biogas yield than the prediction of the first-order model and the transfer function model. Furthermore, the  $B_0$  value obtained by the Cone model was slightly higher than the  $B_0$  value obtained by the other two models. In all models, the variation trend of  $B_0$  was consistent with the variation of measured value. For the nZVI group,  $B_0$  reduced with the increase of dosage. For the  $\text{Fe}_3\text{O}_4$  NPs group, the result showed that  $B_0$  first increased with the dosage and peaked at 1 g  $\text{L}^{-1}$ , then gradually decrease.

Model parameter  $R_m$ , the biogas production rate constant, is often used to evaluate the methane production activity of the reactor. The larger the  $R_m$  within a certain range, the higher the methane production activity. The variation trends of  $B_0$  and  $R_m$  were similar according to Table 4. The  $R_m$  of the nZVI group (1.69–1.90  $\text{L day}^{-1}$ ) and  $\text{Fe}_3\text{O}_4$  NPs group (1.70–1.85  $\text{L day}^{-1}$ ) were higher than that of CK group (1.55  $\text{L day}^{-1}$  for CK1 and 1.56  $\text{L day}^{-1}$  for CK2, respectively) in this study.  $R_m$  was increased by 16.42% and 14.02% in N1 and F2, respectively.

Hydrolysis is the rate-limiting step in the AD process (Ferreira et al., 2014), and the first-order kinetic and the Cone model can calculate the rate of hydrolysis. The parameter  $k$  can be used to characterize the

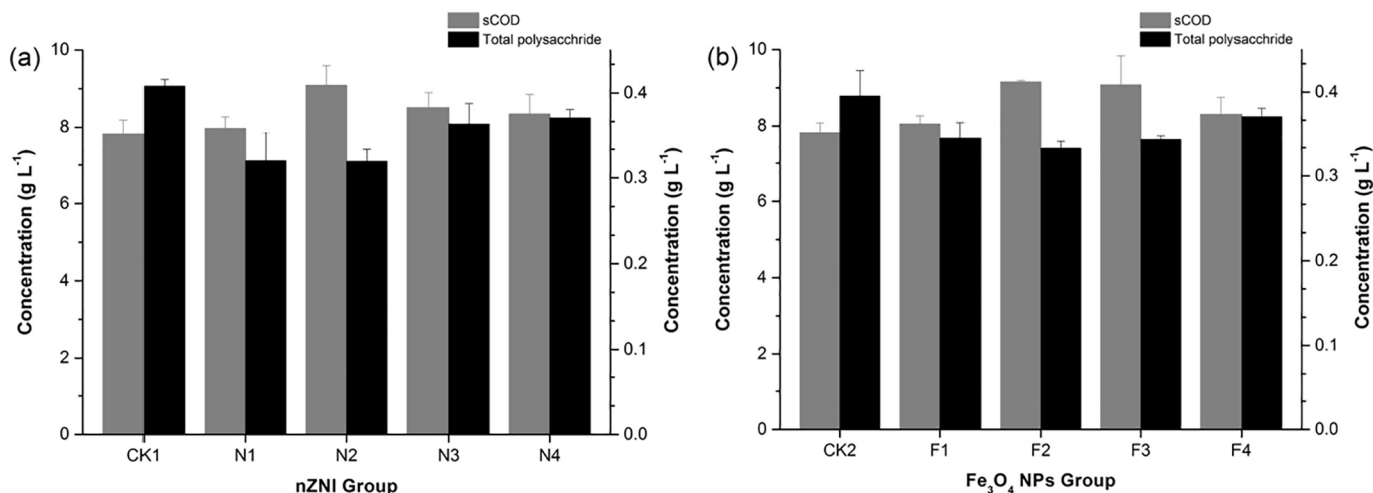


Fig. 6. Changes in sCOD and total polysaccharide after the fermentation for three days.

**Table 3**

Parameters of first-order kinetic model obtained from the biogas production of all CSTRs.

Group	Reactor	R <sup>2</sup>	k	Cumulative methane yield (80 days)				
				Predicted (L)	Measured (L)	rMSPE	AIC	Difference (%)
nZVI	CK1	0.9996	1.22E−04	117.78	121.30	0.79	9.42	2.90
	N1	0.9994	1.12E−03	137.20	140.34	1.16	56.26	2.24
	N2	0.9999	9.85E−04	134.17	137.57	0.42	−78.16	2.47
	N3	0.9995	7.71E−04	131.28	137.09	1.97	48.15	4.24
	N4	0.9999	7.27E−04	133.93	134.44	1.70	−69.01	0.38
	CK2	0.9998	1.46E−04	117.75	120.88	0.68	−27.23	2.59
	F1	0.9998	1.23E−03	130.99	133.53	0.68	−28.10	1.90
	F2	0.9997	1.60E−03	134.35	137.13	0.79	−4.42	2.03
	F3	0.9999	1.58E−03	128.19	131.09	0.53	−59.15	2.22
Fe <sub>3</sub> O <sub>4</sub> NPs	F4	0.9998	6.15E−04	125.78	128.71	0.57	−52.20	2.28

hydrolysis rate of the substrate, the larger the  $k$  value, the higher the degradation rate will be (Zhen et al., 2015b). The  $k$  value calculated by the Cone model was generally slightly higher than that calculated by the first-order model. Considering the  $k$  values obtained by the Cone model as an example, the  $k$  value ranged from 0.0015 to 0.0027 ( $\text{d}^{-1}$ ). The hydrolysis constants of N1 and F2 were highest in the nZVI group and the Fe<sub>3</sub>O<sub>4</sub> NPs group, respectively, with  $k$  value was 0.0027 and 0.0019 ( $\text{d}^{-1}$ ). The fitting result of  $k$  value was consistent with the conclusion that nZVI and Fe<sub>3</sub>O<sub>4</sub> NPs promoted the hydrolysis and acidification of sludge.

Besides the cumulative biogas yield and the hydrolysis rate constant, the lag-phase ( $\lambda$ ), which can be calculated by the transfer function model (Table 4), is also an important parameter to evaluate the behavior of AD process (Zhang et al., 2014). Shorter lag-phase time was found in all reactors. The lag time of nZVI group oscillated between 0.57 and 1.08 (day). As for Fe<sub>3</sub>O<sub>4</sub> group, the lag time ranged from 0.59 to 0.67 (day). The TS content of substrates used in this experiment is low (8.16%), the biogas reactors can be started up quickly, resulting in a shorter lag-phase time. It was interesting to note that the reactors with iron nanoparticles added had longer lag phase than those without iron nanoparticles added, which meant that the presence of nZVI or Fe<sub>3</sub>O<sub>4</sub> NPs delayed the enhancement of biogas yield. It can be explained by the fact that a rapid release of hydrogen could lead to high partial pressure of hydrogen in the nZVI corrosion process. Thus methanogens would be inhibited to a certain extent when the AD just started. Subsequently, the partial pressure of hydrogen decreases due to the consumption of hydrogen methanogens continued to produce methane under the promotion of iron nanoparticles, which could lengthen the lag-phase (Yaobin et al., 2011).

### 3.6. Models evaluation and validation

The properties of both iron nanoparticles and experimental conditions have the important influence on the accuracy and applicability of the model, more dynamic models need to be considered for comparison in the analysis of biogas evolution. To find the best model for evaluating

the biogas production kinetics, the values of R<sup>2</sup>, rMSPE and AIC of three models were calculated and displayed in Table 3–5. The results showed that the Cone model had the highest R<sup>2</sup> value (higher than 0.999) and lowest rMSPE and AIC values among three models, so it was the most suitable model for fitting the anaerobic digestion biogas kinetics in this study. Otherwise, the Cone model achieved minor differences (<1%) between predicted biogas production and measured biogas production (Table 5).

It can be seen that the Cone model fitting experimental biogas yield has high accuracy and applicability because its sigmoidal shape curve could better describe the lag phase, exponential and stable phases in AD process (Li et al., 2015). A similar study has suggested that the Cone model fitting is the best for co-digestion methanogenesis (El-Mashad, 2013). The First-order model only explores the exponential stage of biogas generation and the transfer function model can hardly consider the lag phase as reported by Huilinir et al. (Huiliñir et al., 2014). So, the fitting result of both the first-order model and transfer function model was inferior to that of the Cone model.

## 4. Conclusion

Appropriate addition of nZVI or Fe<sub>3</sub>O<sub>4</sub> NPs is an available technology for enhancing anaerobic digestion performance and biogas yield. The dose of 0.5 g L<sup>−1</sup> nZVI and 1 g L<sup>−1</sup> Fe<sub>3</sub>O<sub>4</sub> NPs had maximal cumulative biogas production after 80 days of semi-continuous AD experiment and reached 140.34 L and 137.13 L, respectively. The results of the three-day fermentation experiment showed that the nZVI or Fe<sub>3</sub>O<sub>4</sub> NPs could promote the acidification-hydrolysis process and ultimately became the fundamental cause of increased methane production. The highest removal ratio of sCOD and VS in the reactor N1 and F2 demonstrated the function of iron nanoparticles in enhancing AD performance. The values of rMSPE and AIC showed that the Cone model was the most suitable model for fitting the measured biogas yields. The kinetic parameters suggested that AD with nZVI or Fe<sub>3</sub>O<sub>4</sub> NPs has higher maximum biogas production rate and higher hydrolysis rate. As the conductive nanoparticles, nZVI and Fe<sub>3</sub>O<sub>4</sub> NPs have the characteristics

**Table 4**

Parameters of transfer function model obtained from the biogas production of all CSTRs.

Group	Reactor	R <sup>2</sup>	Rm	$\lambda$	Cumulative methane yield (80 days)				
					Predicted (L)	Measured (L)	rMSPE	AIC	Difference (%)
nZVI	CK1	0.9997	1.55	0.57	120.89	121.30	0.76	2.57	0.34
	N1	0.9996	1.90	0.92	140.74	140.34	1.04	38.23	0.29
	N2	0.9999	1.86	0.90	137.55	137.57	0.41	−79.95	0.01
	N3	0.9997	1.78	1.06	137.43	137.09	0.87	20.48	0.25
	N4	0.9999	1.69	1.08	134.42	134.44	0.36	−116.98	0.01
	CK2	0.9998	1.56	0.59	120.80	120.88	0.60	−47.60	0.07
	F1	0.9998	1.75	0.64	134.34	133.53	0.65	−34.20	0.61
	F2	0.9998	1.85	0.61	137.74	137.13	0.72	−19.85	0.45
	F3	0.9999	1.74	0.67	131.15	131.09	0.37	−97.08	0.05
Fe <sub>3</sub> O <sub>4</sub> NPs	F4	0.9999	1.70	0.65	128.88	128.71	0.53	−64.88	0.13



**Table 5**

Parameters of Cone model obtained from the biogas production of all CSTRs.

Group	Reactor	R <sup>2</sup>	k	n	Cumulative methane yield (80 days)				
					Predicted (L)	Measured (L)	rMSPE	AIC	Difference (%)
nZVI	CK1	0.9998	1.50E−03	0.99	121.16	121.30	0.65	−28.87	0.12
	N1	0.9997	2.93E−03	1.03	141.09	140.34	0.82	0.85	0.53
	N2	0.9999	2.70E−03	1.08	137.66	137.57	0.39	−94.56	0.07
	N3	0.9999	1.89E−03	1.10	137.82	137.09	0.59	−47.78	0.53
	N4	0.9999	1.79E−03	1.11	134.44	134.44	0.44	−89.59	0.00
	CK2	0.9999	1.53E−03	0.96	120.99	120.88	0.49	−79.79	0.09
	F1	0.9998	1.84E−03	1.05	134.48	133.53	0.58	−47.20	0.72
	F2	0.9998	1.90E−03	1.07	137.94	137.13	0.62	−42.78	0.59
	F3	0.9999	1.77E−04	1.06	131.07	131.09	0.34	−99.95	0.02
	F4	0.9999	1.70E−03	1.04	129.03	128.71	0.46	−90.11	0.25

of providing electrons properties for critical microorganisms in the anaerobic digestion system. This study provides us a new perspective to improve anaerobic digestion process by using other conductive nanoparticles.

Supplementary data to this article can be found online at <https://doi.org/10.1016/j.scitotenv.2019.05.214>.

## Acknowledgements

The study was financially supported by the National Natural Science Foundation of China (51878258, 51578223 and 51521006) and the Key Research and Development Program of Hunan Province (2017SK2242). Finally, we are grateful to Naiqiao Liu for his help in this study.

## References

- Ahmadi-Pirlou M, Ebrahimi-Nik M, Khojastehpour M, Ebrahimi SH. Biodegradation. Mesophilic co-digestion of municipal solid waste and sewage sludge: effect of mixing ratio, total solids, and alkaline pretreatment. *Int. Biodeterior. Biodegradation* 2017; 125: 97–104.
- Banfield, J.F., Zhang, H.Z., 2001. Nanoparticles in the environment. *Reviews in Mineralogy & Geochemistry* 44, 1–58.
- Barua, S., Dhar, B.R., 2017. Advances towards understanding and engineering direct interspecies electron transfer in anaerobic digestion. *Bioresour. Technol.* 244, 698.
- Budiyono, 2010. The influence of total solid contents on biogas yield from cattle manure using rumen fluid inoculum. *Energy Research Journal* 1, 6–11.
- Byrne, J.M., Klueglein, N., Pearce, C., Rosso, K.M., Appel, E., Kappler, A., 2015. Redox cycling of Fe(II) and Fe(III) in magnetite by Fe-metabolizing bacteria. *Science* 347, 1473.
- Capson-Tojo, G., Moscoviz, R., Ruiz, D., Santa-Catalina, G., Trably, E., Rouez, M., et al., 2018. Addition of granular activated carbon and trace elements to favor volatile fatty acid consumption during anaerobic digestion of food waste. *Bioresour. Technol.* 260, 157–168.
- Christopoulos, A., 2006. Fitting Models to Biological Data Using Linear and Nonlinear Regression. *Biometrical J.* 48, 327.
- Eaton, A., 2005. Standard Methods for the Examination of Water and Waste Water.
- El-Mashad, H.M., 2013. Kinetics of methane production from the codigestion of switchgrass and *Spirulina platensis* algae. *Bioresour. Technol.* 132, 305–312.
- Feng, Y., Zhang, Y., Xie, Q., Chen, S., 2014. Enhanced anaerobic digestion of waste activated sludge digestion by the addition of zero valent iron. *Water Res.* 52, 242.
- Ferreira, L.C., Souza, T.S., Fdz-Polanco, F., Pérez-Elvira, S.I., 2014. Thermal steam explosion pretreatment to enhance anaerobic biodegradability of the solid fraction of pig manure. *Bioresour. Technol.* 152, 393–398.
- Gang, L., Wen, W., Irini, A., 2013. Anaerobic digestion for simultaneous sewage sludge treatment and CO biomethanation: process performance and microbial ecology. *Environ Sci Technol* 47, 10685–10693.
- Hassan, M., Ding, W., Shi, Z., Zhao, S., 2016. Methane enhancement through co-digestion of chicken manure and thermo-oxidative cleaved wheat straw with waste activated sludge: a C/N optimization case. *Bioresour. Technol.* 211, 534–541.
- Hassan, Muhammad, Umar, Muhammad, Ding, Weimin, et al., 2017. Methane enhancement through co-digestion of chicken manure and oxidative cleaved wheat straw: stability performance and kinetic modeling perspectives. *Energy* 141, 2314–2320.
- Hu, Y., Hao, X., Dan, Z., Fu, K., 2015. Enhancing the CH<sub>4</sub> yield of anaerobic digestion via endogenous CO<sub>2</sub> fixation by exogenous H<sub>2</sub>. *Chemosphere* 140, 34–39.
- Huiliñir, C., Quintriqueo, A., Antileo, C., Montalvo, S., 2014. Methane production from secondary paper and pulp sludge: effect of natural zeolite and modeling. *Chem. Eng. J.* 257, 131–137.
- Jing, Y., Wan, J., Angelidaki, I., Zhang, S., Luo, G., 2017. iTRAQ quantitative proteomic analysis reveals the pathways for methanation of propionate facilitated by magnetite. *Water Res.* 108, 212–221.
- Karve, A.D., 2003. Cooking without air pollution. *Science* 302, 987.
- Li, H., Chang, J., Liu, P., Fu, L., Ding, D., Lu, Y., 2014. Direct interspecies electron transfer accelerates syntrophic oxidation of butyrate in paddy soil enrichments: syntrophic butyrate oxidation facilitated by nano Fe<sub>3</sub>O<sub>4</sub>. *Environ. Microbiol.* 17 (5).
- Li, K., Liu, R., Sun, C., 2015. Comparison of anaerobic digestion characteristics and kinetics of four livestock manures with different substrate concentrations. *Bioresour. Technol.* 198, 133–140.
- Li, L., Kong, X., Yang, F., Li, D., Yuan, Z., Sun, Y., 2012. Biogas production potential and kinetics of microwave and conventional thermal pretreatment of grass. *Applied Biochemistry & Biotechnology* 166, 1183–1191.
- Luo, J., Feng, L., Chen, Y., Xiang, L., Hong, C., Xiao, N., et al., 2014. Stimulating short-chain fatty acids production from waste activated sludge by nano zero-valent iron. *J. Biotechnol.* 187, 98–105.
- Mao, C., Wang, X., Xi, J., Feng, Y., Ren, G., 2017. Linkage of kinetic parameters with process parameters and operational conditions during anaerobic digestion. *Energy* 135, 352–360.
- McGlynn, S.E., Chadwick, G.L., Kempes, C.P., Orphan, V.J., 2015. Single cell activity reveals direct electron transfer in methanotrophic consortia. *Nature* 526, 531–535.
- Melton, E.D., Swanner, E.D., Sebastian, B., Caroline, S., Andreas, K., 2014. The interplay of microbially mediated and abiotic reactions in the biogeochemical Fe cycle. *Nat. Rev. Microbiol.* 12, 797–808.
- Oleszkiewicz, J.A., Sharma, V.K., 1990. Stimulation and inhibition of anaerobic processes by heavy metals—a review. *Biol. Wastes* 31, 45–67.
- Pan, X., Lv, N., Li, C., Ning, J., Wang, T., Wang, R., et al., 2019. Impact of nano zero valent iron on tetracycline degradation and microbial community succession during anaerobic digestion. *Chem. Eng. J.* 359, 662–671.
- Patricia, T., Rodríguez, J.A., Barba, L.E., Marmolejo, L.F., Pizarro, C.A., 2009. Combined treatment of leachate from sanitary landfill and municipal wastewater by UASB reactors. *Water Science & Technology* 60, 491–495.
- Rotaru, A.-E., Shrestha, P.M., Liu, F., Shrestha, M., Shrestha, D., Embree, M., et al., 2013. A new model for electron flow during anaerobic digestion: direct interspecies electron transfer to Methanosaeta for the reduction of carbon dioxide to methane. *Energy Environ. Sci.* 7 (4), 408–415.
- Shen, C.F., Kosaric, N., Blaszczyk, R., 1993. The effect of selected heavy metals (Ni, Co and Fe) on anaerobic granules and their extracellular polymeric substance (EPS). *Water Res.* 27, 25–33.
- Wang, M., Tang, S.X., Tan, Z.L., 2011. Modeling in vitro gas production kinetics: derivation of logistic-exponential (LE) equations and comparison of models. *Anim Feed Sci Tech* 165, 137–150.
- Wei, W., Cai, Z., Jie, F., Xie, G.J., Li, A., Xu, Z., et al., 1 November 2018. Zero valent iron enhances methane production from primary sludge in anaerobic digestion. *Chem. Eng. J.* 351, 1159–1165.
- Wu, D., Zheng, S., Ding, A., Sun, G., Yang, M., 2015. Performance of a zero valent iron-based anaerobic system in swine wastewater treatment. *J. Hazard. Mater.* 286, 1–6.
- Xiao, X., Guo-Ping, S., Yang, M., Han-Qing, Y.J.W.R., 2013. A modeling approach to describe ZVI-based anaerobic system. *Water Res.* 47, 6007–6013.
- Xie, S., Hai, F.I., Zhan, X., Guo, W., Hao, H.N., Price, W.E., et al., 2016. Anaerobic co-digestion: a critical review of mathematical modelling for performance optimization. *Bioresour. Technol.* 222, 498–512.
- Xu, R., Yang, Z.-H., Wang, Q.-P., Bai, Y., Liu, J.-B., Zheng, Y., et al., 2018a. Rapid startup of thermophilic anaerobic digester to remove tetracycline and sulfonamides resistance genes from sewage sludge. *Sci. Total Environ.* 612, 788–798.
- Xu, R., Yang, Z.H., Zheng, Y., Liu, J.B., Xiong, W.P., Zhang, Y.R., et al., 2018b. Organic loading rate and hydraulic retention time shape distinct ecological networks of anaerobic digestion related microbiome. *Bioresour. Technol.* 262, 184.
- Xu, R., Yang, Z.H., Zheng, Y., Zhang, H.B., Liu, J.B., Xiong, W.P., et al., 2017. Depth-resolved microbial community analyses in the anaerobic co-digester of dewatered sewage sludge with food waste. *Bioresour. Technol.* 244 (Pt 1), 824.
- Yang, G., Zhang, G., Wang, H.J.W.R., 2015. Current state of sludge production, management, treatment and disposal in China. *Water Res.* 78, 60–73.
- Yang, Y., Guo, J., Hu, Z., 2013. Impact of nano zero valent iron (NZVI) on methanogenic activity and population dynamics in anaerobic digestion. *Water Res.* 47, 6790.
- Yang, Z.-H., Xu, R., Zheng, Y., Chen, T., Zhao, L.-J., Li, M., 2016. Characterization of extracellular polymeric substances and microbial diversity in anaerobic co-digestion reactor treated sewage sludge with fat, oil, grease. *Bioresour. Technol.* 212, 164–173.

- Yaobin, Z., Yanwen, J., Xie, Q., Yiwen, L., Pascal, O., 2011. A built-in zero valent iron anaerobic reactor to enhance treatment of azo dye wastewater. *Water Science & Technology* 63, 741–746.
- Zhang, W., Wei, Q., Wu, S., Qi, D., Li, W., Zhuang, Z., et al., 2014. Batch anaerobic co-digestion of pig manure with dewatered sewage sludge under mesophilic conditions. *Appl Energ* 128, 175–183.
- Zhen, G., Lu, X., Kobayashi, T., Kumar, G., Xu, K., 2016. Anaerobic co-digestion on improving methane production from mixed microalgae (*Scenedesmus* sp., *Chlorella* sp.) and food waste: kinetic modeling and synergistic impact evaluation. *Chem. Eng. J.* 299, 332–341.
- Zhen, G., Lu, X., Li, Y.Y., Liu, Y., Zhao, Y., 2015a. Influence of zero valent scrap iron (ZVSI) supply on methane production from waste activated sludge. *Chem. Eng. J.* 263, 461–470.
- Zhen, G.Y., Lu, X.Q., Kobayashi, T., Li, Y.Y., Xu, K.Q., Zhao, Y.C., 2015b. Mesophilic anaerobic co-digestion of waste activated sludge and *Egeria densa*: performance assessment and kinetic analysis. *Appl Energ* 148, 78–86.